

Structural brain alterations in subjects at high-risk of psychosis: A voxel-based morphometric study

E.M. Meisenzahl^{a,*}, N. Koutsouleris^a, C. Gaser^c, R. Bottlender^a,
G.J.E. Schmitt^a, P. McGuire^d, P. Decker^a, B. Burgermeister^a,
C. Born^b, Maximilian Reiser^b, H.-J. Möller^a

^a Department of Psychiatry and Psychotherapy, Ludwig-Maximilians-University, Nussbaumstr. 7, 80336 Munich, Germany

^b Department of Radiology, Ludwig-Maximilians-University, Munich, Germany

^c Department of Psychiatry, Friedrich-Schiller-University, Jena, Germany

^d Department of Psychological Medicine, Institute of Psychiatry, King's College London, UK

Received 26 October 2007; received in revised form 22 February 2008; accepted 22 February 2008

Available online 25 April 2008

Abstract

Forty Untreated high-risk (HR) individuals for psychosis and 75 healthy control subjects (HC) matched for age, gender, handedness and educational level were investigated by structural MRI. HR subjects were recruited at the Early Detection and Intervention Centre for Mental Crises (FETZ) of the Department of Psychiatry and Psychotherapy, Ludwig-Maximilians-University, Germany. Measurements of gray matter volumes were performed by voxel-based morphometry using SPM5. The sample of HR subjects showed GM volume reductions in frontal, lateral temporal and medial temporal regions compared to the healthy control group. These regions are compatible with structural findings in the clinically apparent disease of schizophrenia.

© 2008 Elsevier B.V. All rights reserved.

Keywords: Prodromal psychosis; Imaging; Voxel-based morphometry; Schizophrenia

1. Introduction

In the search of pathogenetic mechanisms underlying the schizophrenic disorder, substantial attention has been given to neurodevelopmental triggers. Neurodevelopmental models are based on a diathesis-stress framework including genetic and environmental risk factors (Andreasen, 1999). These models suggest compromised pre-, perinatal and adolescent brain development as a pivotal factor in the genesis of schizophrenia.

The pathophysiological processes associated with the prodromal state of psychosis have increasingly shifted into the focus of current neuroimaging research. In this context, few recent whole-brain voxel-based morphometric (VBM) studies of high-risk and first-episode populations have provided insight into the neuroanatomical alterations that may evolve before and during the transition from the prodromal phase to the first manifestation of schizophrenia (Borgwardt et al., 2007; Job et al., 2005; Job et al., 2003; Pantelis et al., 2003a). Structural alterations associated with an increased vulnerability to psychosis have been identified mainly within the temporal, perisylvian, limbic and paralimbic structures (Borgwardt et al., 2007; Job et al., 2003). Moreover, this

* Corresponding author.

E-mail address: Eva.Meisenzahl@med.uni-muenchen.de (E.M. Meisenzahl).

vulnerability may express itself early in life by, for example, deviations from the normal cortical gyrification pattern, as shown by Yücel et al. (2003).

Findings from longitudinal MRI studies comparing patients who did and did not subsequently develop psychosis suggest additional alterations in the inferior temporal, limbic and perisylvian regions in the converter group (Borgwardt et al., 2007; Pantelis et al., 2003a). Transition to psychosis may be associated with further structural brain changes within the left hemisphere, including the orbitofrontal region and the anterior cingulate cortex (ACC), the parahippocampus, and the inferior temporal regions (Job et al., 2005; Pantelis et al., 2003a). These structural changes are consistent with studies of first-episode patients (Steen et al., 2006; Vita et al., 2006).

These investigations point to a model of neurobiological vulnerability that develops at different stages of brain maturation, ranging from the pre- and perinatal phase, up to the phase of illness transition (Pantelis et al., 2005). Several authors have shown that young, healthy individuals with a positive familial history for psychotic disorders show subtle neuroanatomical alterations in the hippocampus, the anterior cingulate cortex (ACC) as well as in the prefrontal cortex, possibly as a result of early neurodevelopmental disturbances (Job et al., 2003; Lawrie et al., 1999; Yücel et al., 2003). These findings have been supported by recent results showing that alterations of the prefrontal cortex and the ACC may be associated with genetic and neuropsychological alterations in subjects selected by familial risk factors (McIntosh et al., 2007).

Early neurodevelopmental disturbances may have a negative impact on the subsequent brain maturation, thus provoking accumulating structural alterations in the central nervous system (Pantelis et al., 2005). These late neurodevelopmental lesions could be linked to different precursor states of psychosis that may be characterized clinically by patterns of prepsychotic, attenuated psychotic, or short limited psychotic symptoms (Häfner et al., 2004). Despite considerable progress in understanding the neurobiology of emerging psychosis, it is still unclear which regions of the human cortex are involved structurally in this disease-specific process.

The aim of the study was to compare gray matter volumes in a cross-sectional VBM design including 40 untreated high-risk (HR) individuals for psychosis and 75 healthy control subjects (HC) matched for age, gender, handedness and educational level. We hypothesized that the HR subjects would exhibit gray matter volume reductions compared to HC subjects. For all analyses we used the new unified segmentation model of

SPM5 that possibly provides advantages over the optimized VBM protocol (Good et al., 2001) in detecting subtle morphometric differences in HR subjects compared to the healthy control group.

2. Materials and methods

2.1. Participants

Forty High-risk (HR) individuals (Table 1: mean age \pm SD, 25.0 (5.6), males/females, 25/15) were recruited at the Early Detection and Intervention Centre for Mental Crises (FETZ) of the Department of Psychiatry and Psychotherapy, Ludwig-Maximilians-University, Germany. The FETZ participated in a prospective high-risk multi-center study within the German Research Network on

Table 1
Statistical analysis of sociodemographic, clinical and global anatomical parameters of HC and HR groups

Parameters	HC	HR	T/χ^2	P
Count	75	40		
Gender				
(% subjects in group)				
Male	46 (61)	25 (63)	0.02 ^a	0.533
Female	29 (39)	15 (38)		
Age				
Mean years (SD)	25.1 (3.80)	25.0 (5.59)	0.146 ^b	0.831
Educational years				
Mean years (SD)	12.21 (1.81)	12.05 (1.26)	1.42 ^b	0.160
Handedness				
(% subjects in group)				
Right	67 (89)	36 (90)	0.75 ^a	0.687
Left	6 (8)	2 (5)		
Ambidextruous	2 (3)	2 (5)		
PANSS				
Sum score	–	52.6 (15.2)		
Positive Symptoms	–	10.7 (3.3)		
Negative Symptoms	–	13.3 (6.6)		
General Psychopathology	–	28.7 (7.8)		
Global anatomical parameters [mm ³]				
Gray matter volume	654.6 (73.8)	676.2 (71.6)	–1.51	0.134
White matter volume	520.7 (65.8)	525.7 (57.1)	–0.40	0.688
CSF volume	459.6 (98.5)	461.6 (92.5)	–0.11	0.916
Total intracranial volume	1634.9 (204.0)	1663.5 (167.7)	–0.75	0.453
Distance ² to mean voxel value in GM (SD)* 10 ³	146.0 (9.1)	146.1 (8.9)	–0.81	0.851

Significance threshold defined at $P < 0.05$.

^a Pearson's χ^2 value.

^b T test.

Schizophrenia (Häfner et al., 2004). Potential HR subjects were referred to the FETZ by primary health care services and were examined by means of a standardized inclusion criteria checklist (ICC) using operationalized definitions of different types of prodromal symptoms: (1) basic symptoms (thought interferences, thought perseveration, thought pressure, thought blockages, disturbances of receptive language, decreased ability to discriminate between ideas and perception, unstable ideas of reference (subject-centrism), derealization, visual perception disturbances, acoustic perception disturbances) taken from the Bonn Scale for Assessment of Prodromal Symptoms (BSABS) (Klosterkötter et al., 2001; Kojoh and Hirasawa, 1990), (2) attenuated psychotic (APS) and brief limited psychotic symptoms (BLIPS) as defined by the UHR criteria of the Personal Assessment and Crisis Evaluation (PACE) clinic in Melbourne (Yung et al., 2003; Yung et al., 2004). Furthermore, subjects' psychopathology was evaluated by means of the Positive and Negative Syndrome Scale (PANSS). The premorbid IQ of the HR subjects was assessed using the MWT-B, an established instrument in German-speaking populations (Lehrl, 2005). All subjects had never received neuroleptic agents prior to MRI and clinical examination.

The medical and psychiatric history of HR and all other subjects (see below) was assessed by means of a standardized and structured clinical interview as well as with the Standardized Clinical Interview for DSM-IV. Potential HR subjects meeting defined sets of state and/or trait markers were included in the study. Inclusion based on global functioning and trait factors required a >30 point reduction in the DSM-IV Global Assessment of Functioning (GAF) Scale and (1) a familial history of psychotic disorders in the first-degree relatives, or (2) a personal history of pre-/perinatal complications. Inclusion based on psychopathological state markers required at least 1 positive item in the prodromal symptom categories of the ICC.

Exclusion criteria were (1) transition to psychosis as defined by Yung et al. (1998), (2) a past or present diagnosis of schizophrenia spectrum and bipolar disorders, as well as delirium, dementia, amnesic or other cognitive disorders, mental retardation and psychiatric disorders due to a somatic factor or related to psychotropic substances, following the DSM-IV criteria, (3) alcohol or drug abuse according to DSM-IV within three months prior to examination, and (4) past or present inflammatory, traumatic or epileptic diseases of the central nervous system.

A regular clinical follow-up was performed in monthly intervals during the first year and quarterly in the following 3 years. At each assessment, subjects were

re-evaluated using the ICC in order to detect a possible transition to psychosis (Yung et al., 1998). In subjects meeting the transition criteria the diagnosis of schizophrenia spectrum disorders was determined using the ICD-10 diagnostic research criteria at time of transition and after 1 year.

In addition, 75 healthy control (HC) subjects matched group-wise to the HR group for age, gender, handedness and educational years (Table 2: mean age \pm SD, 25.1 (3.8), males/females, 46/29) were recruited for MRI examination. Only those HC were included in the study that had no past or present personal or familial history (1st degree relatives) of neurological and/or psychiatric conditions.

2.2. MRI data acquisition

MR images were obtained on a 1.5T Magnetom Vision scanner (Siemens, Erlangen, Germany). Subjects were scanned with a T1-weighted 3D-MPRAGE sequence (TR, 11.6 ms; TE, 4.9 ms; field of view, 230 mm; matrix, 512 \times 512; 126 contiguous axial slices of 1.5 mm thickness; voxel size, 0.45 \times 0.45 \times 1.5 mm). Every scan was checked for image artifacts and gross anatomical abnormalities. Data analysis was performed using the SPM5 software package (Wellcome Department of Cognitive Neurology, London, UK) running under MATLAB 2007a (The MathWorks, Natick, MA, USA).

2.3. MRI data preprocessing

The present study employed the VBM5 toolbox (<http://dbm.neuro.uni-jena.de>), which utilizes and extends the new unified segmentation approach implemented in SPM (Ashburner and Friston, 2005). Unified segmentation provides a generative model of VBM preprocessing that integrates tissue classification, image registration and MRI inhomogeneity bias correction. Thus, the model avoids the "circularity problem" of the optimized VBM procedure (Good et al., 2001), as the initial image registration does not require an initial tissue segmentation and vice versa. The VBM5 toolbox extends the unified segmentation model as it increases the quality of segmentation by applying a Hidden Markov Field (HMRF) model on the segmented tissue maps (Bach Cuadra et al., 2005). The HMRF algorithm provides spatial constraints based on neighbouring voxel intensities within a 3 \times 3 \times 3 voxel cube. It removes isolated voxels which are unlikely to be a member of a certain tissue class and also closes holes in a cluster of connected voxels of a certain class resulting

Table 2
Cross-sectional VBM analysis of GM volume reductions in HR vs HC (HC>HR)

Anatomical region	LEFT				RIGHT			
	Extent	T	D	%diff	Extent	T	D	%diff
	<i>k</i> (%clust; %reg)	Max; mean (SD)	Max; mean (SD)	Max; mean (SD)	<i>k</i> (%clust; %reg)	Max; mean (SD)	Max; mean (SD)	Max; mean (SD)
<i>Cluster 1: k_c = 91,048; P_{cFWE} < .000; Voxel maximum: x,y,z [mm] = 48,38,18; P_{FWE} = 0.044</i>								
Caudate	901 (1.0; 11.7)	3.24; 2.64 (0.19)	0.62; 0.50 (0.04)	-2.21; -2.35 (0.25)	136 (0.2; 1.7)	2.97; 2.57 (0.16)	0.57; 0.49 (0.03)	-2.06; -2.07 (0.08)
Cingulum Ant	3990 (4.4; 35.6)	3.68; 2.82 (0.31)	0.70; 0.54 (0.06)	-2.59; -2.44 (0.43)	5418 (6.0; 51.6)	4.20; 2.93 (0.38)	0.80; 0.56 (0.07)	-3.48; -2.60 (0.46)
Cingulum Mid	501 (0.6; 3.2)	3.23; 2.59 (0.19)	0.62; 0.49 (0.04)	-2.32; -1.92 (0.18)	926 (1.0; 5.3)	3.92; 2.72 (0.37)	0.75; 0.52 (0.07)	-2.67; -2.06 (0.24)
Frontal Inf Oper					617 (0.7; 5.5)	4.09; 2.72 (0.37)	0.78; 0.52 (0.07)	-2.63; -1.96 (0.42)
Frontal Inf Orb					230 (0.3; 1.7)	3.53; 2.78 (0.32)	0.67; 0.53 (0.06)	-1.63; -1.40 (0.17)
Frontal Inf Tri					3425 (3.8; 19.9)	4.68; 3.17 (0.52)	0.89; 0.60 (0.10)	-2.39; -2.20 (0.64)
Frontal Mid	1893 (2.1; 4.9)	3.72; 2.76 (0.27)	0.71; 0.53 (0.05)	-2.38; -1.85 (0.28)	14000 (15.4; 34.3)	4.97; 3.05 (0.56)	0.95; 0.58 (0.11)	-2.46; -2.04 (0.48)
Frontal Mid Orb					1699 (1.9; 20.9)	3.95; 2.84 (0.36)	0.75; 0.54 (0.07)	-2.10; -1.74 (0.22)
Frontal Med Orb	3578 (3.9; 62.2)	4.12; 3.03 (0.39)	0.79; 0.58 (0.07)	-2.57; -2.39 (0.46)	3819 (4.2; 55.8)	4.30; 2.92 (0.40)	0.82; 0.56 (0.08)	-3.63; -2.45 (0.51)
Frontal Sup	3140 (3.5; 10.9)	3.73; 2.80 (0.30)	0.71; 0.53 (0.06)	-2.47; -1.97 (0.30)	8278 (9.1; 25.5)	4.70; 2.97 (0.49)	0.90; 0.57 (0.09)	-3.21; -2.12 (0.35)
Frontal Sup Med	13844 (15.2; 57.8)	4.93; 3.12 (0.53)	0.94; 0.60 (0.10)	-2.78; -2.21 (0.42)	11211 (12.3; 65.7)	4.31; 3.10 (0.46)	0.82; 0.59 (0.09)	-2.68; -2.24 (0.42)
Frontal Sup Orb	82 (0.1; 1.1)	2.78; 2.48 (0.10)	0.53; 0.47 (0.02)	-1.70; -1.53 (0.09)	1624 (1.8; 20.4)	3.50; 2.78 (0.29)	0.67; 0.53 (0.05)	-2.35; -1.95 (0.26)
Olfactory	102 (0.1; 4.6)	3.11; 2.64 (0.20)	0.59; 0.50 (0.04)	-2.05; -1.94 (0.12)	247 (0.3; 10.7)	2.99; 2.61 (0.16)	0.57; 0.50 (0.03)	-1.96; -1.95 (0.11)
Precentral	538 (0.6; 1.9)	3.17; 2.63 (0.20)	0.60; 0.50 (0.04)	-2.15; -2.04 (0.35)	1479 (1.6; 5.5)	4.24; 3.03 (0.49)	0.81; 0.58 (0.09)	-4.27; -2.80 (0.81)
Rectus	2695 (3.0; 39.5)	4.05; 2.82 (0.37)	0.77; 0.54 (0.07)	-2.49; -1.92 (0.33)	1561 (1.7; 26.2)	3.43; 2.73 (0.26)	0.65; 0.52 (0.05)	-2.36; -1.76 (0.35)
Supp Motor Area	2001 (2.2; 11.7)	3.30; 2.65 (0.22)	0.63; 0.50 (0.04)	-2.34; -2.01 (0.20)	1525 (1.7; 8.0)	3.48; 2.79 (0.29)	0.66; 0.53 (0.06)	-2.52; -2.15 (0.23)
<i>Cluster 2: k_c = 9179; P_{cFWE} = 0.002; Voxel maximum: x,y,z [mm] = -60, -39, 2; P_{FWE} = 0.116</i>								
Heschl	51 (0.6; 2.8)	3.90; 2.94 (0.34)	0.45; 0.48 (0.02)	-1.38; -1.53 (0.10)				
Rolandic Oper	23 (0.3; 0.3)	3.68; 2.99 (0.41)	0.61; 0.58 (0.06)	-2.03; -1.98 (0.32)				
Postcentral	261 (2.8; 0.8)	3.66; 2.86 (0.34)	0.51; 0.51 (0.04)	-1.68; -1.69 (0.24)				
SupraMarginal	830 (9.0; 8.3)	3.95; 2.87 (0.35)	0.50; 0.54 (0.07)	-1.70; -1.91 (0.27)				
Temporal Mid	4133 (45.0; 10.5)	4.05; 2.79 (0.35)	0.47; 0.58 (0.10)	-1.59; -2.38 (0.58)				
Temporal Sup	3868 (42.1; 21.1)	4.12; 2.93 (0.40)	0.49; 0.54 (0.07)	-1.69; -2.07 (0.31)				
<i>Cluster 3: k_c = 15,946; P_{cFWE} < 0.000; Voxel maximum: x,y,z [mm] = -50, 15, 34; P_{FWE} = 0.127</i>								
Frontal Inf Oper	1309 (8.2; 15.8)	4.04; 2.91 (0.38)	0.48; 0.56 (0.11)	-1.94; -2.00 (0.34)				
Frontal Inf Tri	5132 (32.2; 25.4)	4.12; 2.77 (0.37)	0.61; 0.56 (0.08)	-2.21; -1.96 (0.45)				
Frontal Mid	8204 (51.5; 21.1)	4.05; 2.91 (0.38)	0.52; 0.53 (0.07)	-1.78; -1.77 (0.25)				
Frontal Sup	68 (0.4; 0.2)	3.62; 2.97 (0.31)	0.46; 0.48 (0.02)	-1.43; -1.48 (0.10)				
Precentral	1234 (7.7; 4.4)	3.98; 2.93 (0.36)	0.46; 0.57 (0.09)	-1.36; -1.94 (0.30)				
<i>Cluster 4: k_c = 7593; P_{cFWE} = 0.007; Voxel maximum: x,y,z [mm] = 44, -11, -14; P_{FWE} = 0.368</i>								
Insula					52 (0.7; 0.4)	4.12; 2.95 (0.43)	0.49; 0.50 (0.04)	-1.51; -1.52 (0.09)
Temporal Inf					825 (10.9; 2.9)	3.75; 2.58 (0.19)	0.55; 0.52 (0.05)	-2.62; -2.34 (0.21)
Temporal Mid					2129 (28.0; 6.0)	4.04; 2.83 (0.35)	0.52; 0.52 (0.06)	-2.00; -2.35 (0.45)
Temporal Sup					3913 (51.5; 15.6)	4.10; 2.91 (0.39)	0.55; 0.53 (0.07)	-1.66; -2.13 (0.34)
<i>Cluster 5: k_c = 8300; P_{cFWE} = 0.004; Voxel maximum: x,y,z [mm] = -42, 49, -10; P_{FWE} = 0.993</i>								
Insula	1890 (22.8; 12.7)	4.04; 2.94 (0.41)	0.52; 0.50 (0.03)	-2.53; -1.82 (0.27)				
Frontal Inf Oper	43 (0.5; 0.5)	3.80; 3.03 (0.41)	0.47; 0.47 (0.02)	-1.49; -1.61 (0.11)				
Frontal Inf Orb	1808 (21.8; 13.4)	4.05; 2.73 (0.33)	0.47; 0.51 (0.04)	-2.05; -1.67 (0.22)				
Frontal Inf Tri	203 (2.5; 1.0)	4.12; 2.94 (0.47)	0.53; 0.51 (0.03)	-2.48; -2.28 (0.34)				
Frontal Mid	88 (1.1; 0.2)	4.02; 2.99 (0.53)	0.47; 0.47 (0.02)	-1.79; -1.72 (0.33)				
Frontal Mid Orb	2172 (26.2; 30.6)	4.04; 2.79 (0.34)	0.47; 0.51 (0.04)	-1.33; -1.68 (0.24)				
Frontal Sup	971 (11.7; 3.4)	4.06; 2.88 (0.42)	0.49; 0.51 (0.04)	-1.88; -2.26 (0.36)				
Frontal Sup Orb	1102 (13.3; 14.3)	4.04; 2.88 (0.34)	0.48; 0.50 (0.04)	-2.25; -2.02 (0.25)				

Clusters were characterized by their extent *k_c* and significance *P_{cFWE}*, corrected for cluster extent and smoothness non-stationarity, as well as by the localisation *x,y,z* [mm] and corrected *P_{FWE}* value of the maximum voxel. For anatomical regions within clusters, the number of voxels *k*, the percentage of the cluster covered by the region %clust, the percentage of the region covered by the cluster %reg, the max; mean (SD) of effect sizes *D* and the percental differences of GM volume %diff were reported.

Abbreviations: *Ant* Anterior, *Front* Frontal, *Inf* Inferior, *Med* Medial, *Mid* Middle, *Oper* Opercular, *Orb* Orbital, *Tri* Triangular, *Sup* Superior, *Supp* Supplementary.

in a higher signal-to-noise ratio of the final tissue probability maps. SPM5 writes the estimated tissue maps by using Bayes rule for combining the likelihood of certain voxels belonging to a tissue class with the *a priori* knowledge of the respective ICBM tissue prior (International Consortium for Brain Mapping). However, these tissue priors are derived from the brains of healthy subjects with a mean age of 25 years. Thus, a segmentation bias may be introduced in the final tissue maps of study populations that deviate anatomically from these healthy subjects, e.g. schizophrenic patients, who frequently show ventricular enlargement. In order to avoid such bias the VBM5 toolbox offers the possibility to write the estimated tissue probability maps without making use of the priors.

We used this option as it improved the delineation of subcortical structures and sulci. The final tissue maps of gray matter (GM), white matter (WM) and cerebro-spinal fluid (CSF) were modulated with the Jacobian determinants of the deformation parameters obtained by normalization to the MNI standard space (Montreal Neurological Institute) in order to analyze volume differences between study populations. Finally, the modulated GM partitions were smoothed with a 10 mm FWHM Gaussian kernel and entered statistical analysis.

Additionally, global GM, WM and CSF volumes as well as total intracranial volumes were computed using the native-space tissue maps of each subject. Moreover, the anatomical heterogeneity was compared between samples by calculating the squared distance of each subject's normalized GM tissue map to the sample mean using the VBM5 toolbox (Table 2).

2.4. Statistical analysis

By employing the General Linear Model an analysis of covariance (AnCova) was designed in order to investigate focal GM volume differences between the HC and HR groups. Global GM volume, age and gender were entered as covariates of no interest in the statistical design. GM volume differences (reductions, increments) between the HR and HC samples were investigated using the following *T* contrasts: [HC>HR] for GM volume reductions in the HR sample versus HC and [HC<HR] for GM volume increments in the HR sample versus HC.

Statistical inference was performed at the cluster-level by assessing the SPM{t} images using the non-stationary random field theory (Hayasaka et al., 2004). Cluster-size statistics have shown to be more sensitive to spatially extended signals compared to voxel-intensity methods (Poline et al., 1997). Moreover, this methodology mitigates the multiple-comparison problem inherent

in mass-univariate statistical tests. However, the use of cluster-size tests in VBM was invalid until recently (Ashburner and Friston, 2000) as structural MRI images violate the parametric test assumption of uniform smoothness, thus biasing cluster-size tests towards an increased false positive rate in smoother regions and reduced statistical power in rougher regions (Worsley et al., 1999). This problem can be addressed by adjusting cluster sizes according to the local smoothness (FWHM) at each voxel within the framework of the Random Field Theory (RFT) (Cao and Worsley, 2001; Hayasaka et al., 2004; Worsley et al., 1999). Non-stationary RFT cluster-based inference has proven to be robust for MRI experiments that fulfill the following requirements: (1) degrees of freedom $df > 30$ and (2) image smoothness (FWHM) $> 3 \times$ voxel sampling resolution (Hayasaka et al., 2004). Both requirements were met by the present study.

Our inference procedure started with the definition of a primary threshold in order to identify contiguous voxels for the cluster-level analysis at a relatively lenient voxel level (Nichols and Holmes, 2002). Low primary thresholds ($P > 0.05$, uncorrected) may sensitize the cluster test for spatially extended, low-signal clusters at the price of spatial resolution, whereas high ($P < 0.001$, uncorrected) thresholds may produce a higher spatial cluster resolution at the cost of spatial extent. In the present study the primary threshold was set to $P < 0.01$, uncorrected, in order to find a compromise between sensitivity to cluster extent and separation of maximal voxel results. Then, a family-wise-error corrected (FWE) cluster-size threshold of $P < 0.05$ was applied that produced a spatial extent threshold of 5.2 cm^3 . Finally, cluster sizes were adjusted for smoothness non-uniformity by means of the VBM5 toolbox which implements the methodology of Hayasaka et al. (2004). Anatomical regions covered by significant clusters were identified using Automated Anatomical Labeling (AAL) (Tzourio-Mazoyer et al., 2002). GM differences in these regions were quantified by calculating the effect sizes (Cohen's *D*) of the SPM{t} maps and by extracting the percental between-group differences (%diff) from the contrast images.

An additional VBM analysis was carried out in order to assess the relationships between the PANSS positive and negative scores and GM volume in the HR sample. Therefore, a multiple regression design was constructed that included two regressor variables with the individual scores in the PANSS positive and negative subscales, controlling for age, gender and global GM volume. The described cluster-based inference strategy was employed in order to assess correlations between GM

volume and psychopathology: the primary threshold was set to $P < 0.01$, uncorrected. Then, the FWE-corrected cluster-extent threshold of $P < 0.05$ defined a minimum cluster size of 4.25 cm^3 . Furthermore, the correlation coefficients were computed for voxels within significant clusters using the VBM5 toolbox.

3. Results

3.1. Sociodemographic and clinical parameters

No significant differences regarding age, gender, handedness and educational years were observed

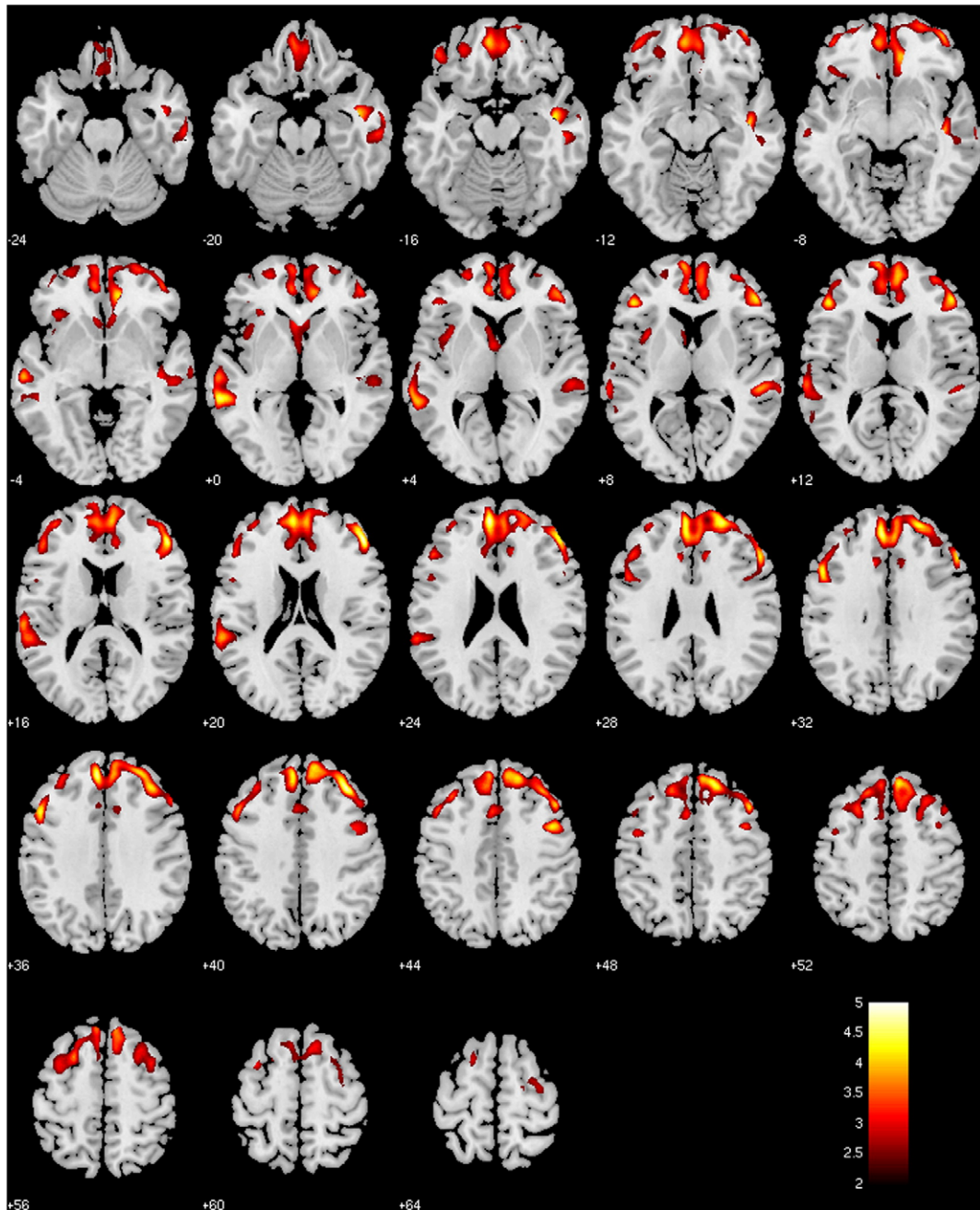


Fig. 1. Significant GM volume decreases [HC > HR] in HR versus HC at $P < 0.05$, FWE-corrected cluster-size threshold. Global gray matter volume, age and gender were modeled as covariates of no interest in the statistical design. T values of voxels within significant clusters were overlaid on the MNI single subject template.

between the HC and HR samples. PANSS scale ratings were given in Table 1. The mean (SD) premorbid IQ of the HR sample was 109.0 (15.0). In the HR sample, 69.8% of subjects had a GAF reduction of >30 points at MRI scan. 11.9%/16.7% of our HR populations had a first-degree relative with affective psychosis/schizophrenic psychosis.

Thirty-three HR subjects completed the four-year follow-up period, of whom fifteen transitioned to psychosis. The mean (min–max) time to transition was 188 (35–777) days. Thirteen subjects developed psychosis during the first year of follow-up, one subject in the second and one in the third year. The ICD-10 diagnoses in the transitioned HR subjects were as follows: schizophrenia ($n=9$), schizoaffective psychosis ($n=5$) and schizotypal personality disorder ($n=1$). Seven dropped from the study as they refused to participate or because they could not be contacted. 26.7% of the 15 transitioned HR subjects compared to 17.6% ($P=0.678$, Fisher's exact test) of the non-transitioned HR subgroup had a positive family history of schizophrenia spectrum psychoses in the first-degree relatives. A positive history of pre- and perinatal complication was detected in 40.0% of converters versus 31.3% of non-converters ($P=0.716$, Fisher's exact test). The converters scored significantly higher on the PANSS

positive scale relative to the non-converters (mean (SD): 12.9 (4.5) versus 10.0 (2.4), $P=0.029$, Student's t test). All 15 converters had a GAF reduction of >30 points, whereas this was the case only in 55.6% of the non-converters ($P=0.004$, Fisher's exact test).

3.2. VBM analysis: HC versus HR

Global brain volumes did not differ between the two groups (statistical level $P<0.05$, Table 1). At $P<0.05$, cluster-level corrected, 5 clusters of GM volume reductions in HR compared to HC were identified within the frontal and temporal brain regions (Table 2, Fig. 1):

- (1) A large prefrontal cluster (cluster 1, $k_c=91,048$, $P_{\text{CFWE}}<0.000$) involving the dorsomedial and ventromedial prefrontal cortex (DMPFC, VMPFC), the bilateral dorsolateral and right ventrolateral prefrontal (DLPFC, VLPFC) cortex, the orbitofrontal cortex (OFC) and the anterior cingulate cortex (ACC). This cluster extended into the caudate nuclei, olfactory areas, the precentral gyri and the supplementary motor areas, bilaterally. The effect sizes within this cluster were medium to large,

Table 3
Correlational VBM analysis of GM volume and individual PANSS scores

Anatomical region	Left			Right		
	Extent	T	C	Extent	T	C
	k (%clust; %reg)	Max; mean (SD)	Max; mean (SD)	k (%clust; %reg)	Max; mean (SD)	Max; mean (SD)
<i>Negative correlation: GM volume and PANSS positive score</i>						
Cluster 1: $k=7196$; $P_{\text{CFWE}}<0.003$; Voxel maximum (x,y,z [mm]): 8,37,14; $P_{\text{FWE}}=0.982$						
Frontal Sup Med	994 (13.8; 4.2)	3.87; 2.84 (0.25)	0.65; 0.54 (0.03)	2861 (39.8; 27.2)	4.40; 3.18 (0.45)	0.70; 0.58 (0.05)
Cingulum Ant	2880 (40.0; 25.7)	3.61; 2.84 (0.23)	0.63; 0.54 (0.03)			
<i>Negative correlation: GM volume and PANSS negative score</i>						
Cluster 1: $k=6967$; $P_{\text{CFWE}}=0.003$; Voxel maximum (x,y,z [mm]): 5, 61, 21; $P_{\text{FWE}}=0.747$						
Frontal Sup Med	4703 (67.5; 19.7)	4.42; 3.01 (0.37)	0.66; 0.56 (0.05)	2203 (31.6; 12.9)	4.48; 3.04 (0.40)	0.59; 0.57 (0.06)
Frontal Med Orb	20 (0.3; 0.4)	2.94; 2.73 (0.12)	0.50; 0.50 (0.01)			
Cingulum Ant	20 (0.3; 0.2)	3.33; 2.97 (0.23)	0.50; 0.51 (0.02)			
Cluster 2: $k=16490$; $P_{\text{CFWE}}<0.000$; Voxel maximum (x,y,z [mm]): -38, 52, 11; $P_{\text{FWE}}=0.969$						
Precentral	2994 (18.2; 10.6)	3.79; 2.92 (0.29)	0.65; 0.54 (0.04)			
Frontal Mid	6028 (36.6; 15.5)	4.48; 3.07 (0.42)	0.71; 0.56 (0.05)			
Frontal Inf Oper	466 (2.8; 5.6)	4.26; 3.10 (0.46)	0.69; 0.57 (0.05)			
Frontal Inf Tri	6840 (41.5; 33.8)	4.06; 2.94 (0.31)	0.67; 0.55 (0.04)			
Frontal Inf Orb	160 (1.0; 1.2)	3.41; 2.86 (0.23)	0.61; 0.54 (0.03)			
Cluster 3: $k=4330$; $P_{\text{CFWE}}=0.047$; Voxel maximum (x,y,z [mm]): 45, 49, 7; $P_{\text{FWE}}=0.999$						
Frontal Mid	3279 (75.7; 8.0)	4.42; 2.95 (0.33)	0.61; 0.55 (0.04)			
Frontal Inf Tri	1048 (24.2; 6.1)	4.34; 3.05 (0.41)	0.55; 0.54 (0.03)			

Clusters were characterized by their extent k_c and significance P_{CFWE} , corrected for non-stationarity, as well as by the localisation x,y,z [mm] and corrected P_{FWE} value of the maximum voxel. For anatomical regions within clusters, the number of voxels k , the percentage of the cluster covered by the region %clust, the percentage of the region covered by the cluster %reg, the max; mean (SD) of correlations coefficients C were reported.

Abbreviations: *Ant* Anterior, *Front* Frontal, *Inf* Inferior, *Med* Medial, *Mid* Middle, *Oper* Opercular, *Orb* Orbital, *Tri* Triangular, *Sup* Superior, *Supp* Supplementary.

ranging from 0.53 (left OFC) to 0.95 (right DLPFC). The percental GM differences lay between -1.7% (left OFC) and -4.3% (right precentral gyrus).

(2) A further left-hemispheric cluster covering portions of the VLPFC, DLPFC and precentral gyrus (cluster 3, $k_c=15,946$, $P_{cFWE}<0.000$). The maximum effect size was found in the VLPFC

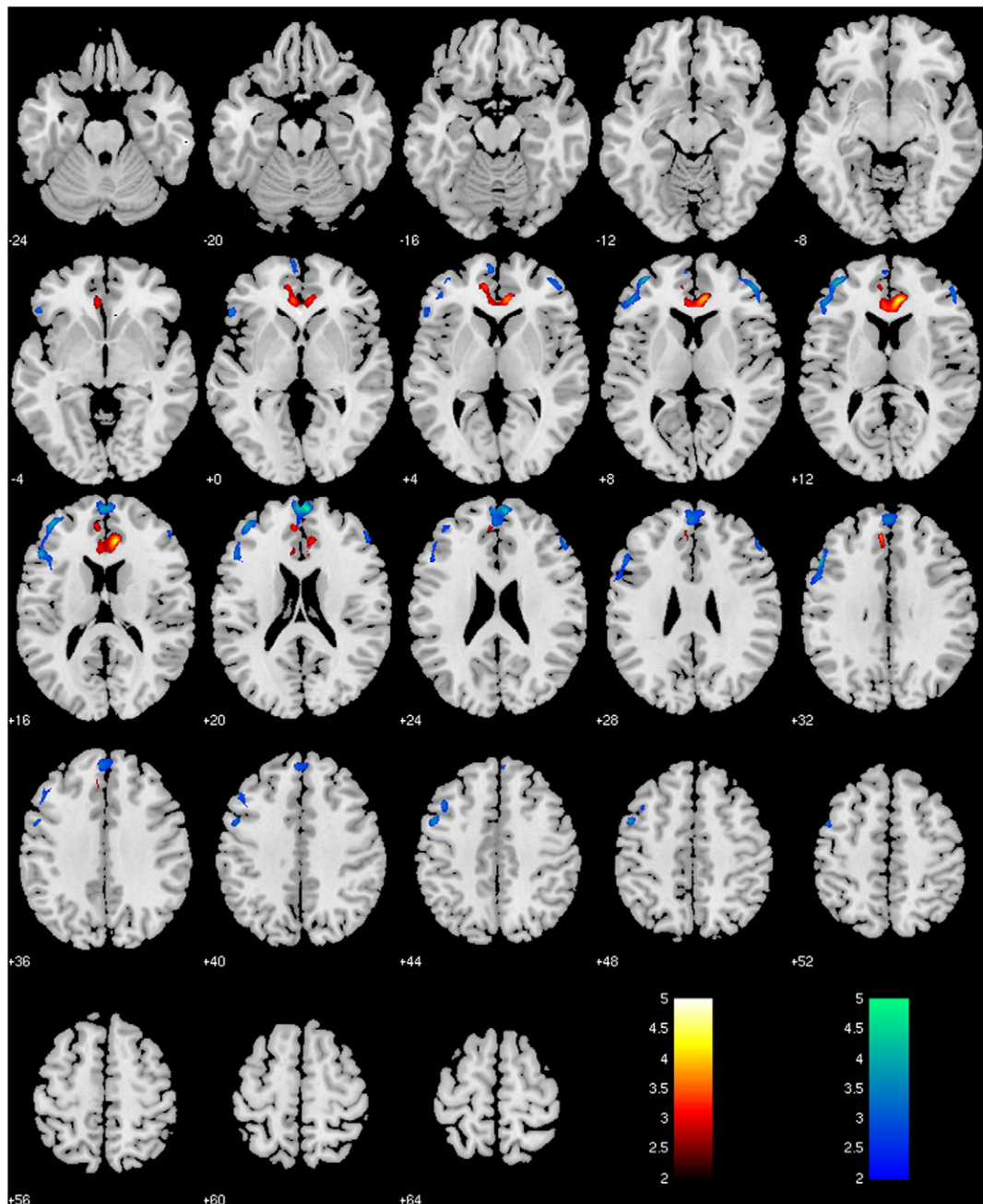


Fig. 2. Significant inverse correlations between GM volume and PANSS positive (warm color scale) and negative (cool color scale) at $P<0.05$, FWE-corrected cluster-size threshold. Global gray matter volume, age and gender were modeled as covariates of no interest in the statistical design. T values of voxels within significant clusters were overlaid on the MNI single subject template. (For interpretation of the references to color in this figure legend, the reader is referred to the web version of this article.)

($D=0.61$) with a maximum percental difference of -2.21% .

- (3) A third prefrontal cluster on the left hemisphere occupying the VLPFC, DLPFC and extending to the OFC and insular cortex (cluster 5, $k_c=8300$, $P_{\text{cFWE}}=0.004$). The effect sizes/percental GM differences lay between $0.47/-1.33\%$ (OFC) and $0.53/-2.48\%$ (VLPFC).
- (4) A left-sided cluster (cluster 2, $k_c=9179$, $P_{\text{cFWE}}=0.002$) covering the middle temporal gyrus as well as the perisylvian region (superior temporal gyrus (STG), supramarginal gyrus, postcentral gyrus and Rolandic operculum). The effect sizes/percental GM differences ranged from $0.45/-1.38\%$ (Heschl gyrus) to $0.61/-2.03\%$ (Rolandic operculum).
- (5) A right-sided temporal cluster (cluster 4, $k_c=7593$, $P_{\text{cFWE}}=0.007$) involving the insular cortex, the inferior, middle and superior temporal gyrus. The maximum effect size was found in the inferior temporal gyrus ($D=0.55$) with a maximum percental difference of -2.62% .

3.3. VBM analysis: correlations between GM volume and PANSS scores

Significant inverse correlations between GM volume and the PANSS positive symptom scores were identified within a medial prefrontal cluster ($k_c=7196$, $P_{\text{cFWE}}=0.003$; Table 3, Fig. 2) that covered parts of the DMPFC, bilaterally and the left ACC. The maximum correlation coefficients within this cluster ranged from -0.63 in the ACC to -0.70 in the right DMPFC.

Significant inverse correlations between GM volume and the PANSS negative symptom scores were identified in three prefrontal cluster located within the medial and lateral prefrontal cortices:

- (1) A medial prefrontal cluster ($k_c=6967$, $P_{\text{cFWE}}=0.003$; Table 3, Fig. 2) that mainly occupied portions of the DMPFC, bilaterally and extended to the left ACC and OFC. The maximum correlation coefficients within this cluster were found in the DMPFC ($C=-0.66$).
- (2) An extended left-hemispheric cluster ($k_{\text{ccd/med}}=16,490$, $P_{\text{cFWE}}<0.000$; Table 3, Fig. 2) including parts of the VLPFC and DLPFC with extensions to the precentral gyrus and OFC. The correlation coefficient maximum was identified in the left DLPFC ($C=0.71$).
- (3) A smaller left-hemispheric cluster ($k_c=4330$, $P_{\text{cFWE}}<0.000$; Table 3, Fig. 2) localized in the

DLPFC and VLPFC with maximum correlations of $C=0.61$.

4. Discussion

The aim of the study was to compare GM volumes in a cross-sectional VBM design of 40 untreated high-risk (HR) individuals for schizophrenia with 75 matched healthy control subjects. We hypothesized that the HR group would show structural reductions of GM volume compared to HC subjects.

In the past, different neurodevelopmental models have been formulated, emphasizing the possible role of early (Weinberger, 1987) or late (Benes, 1991; McGlashan and Hoffman, 2000) neurodevelopmental lesions in the pathophysiology of psychosis. Recently, Pantelis et al. (2003b, 2005) united both perspectives into an integrative neurodevelopmental model of schizophrenia.

Our VBM results confirmed the assumed structural changes in HR subjects compared to HC subjects. In order to be comparable to previous cross-sectional VBM studies of HR subjects (Borgwardt et al., 2007; Job et al., 2003; Pantelis et al., 2003a) we used cluster-based statistical inference together with non-stationarity correction (Hayasaka et al., 2004) capable of detecting subtle and spatially extended brain alterations, which otherwise may have been missed by a voxel-based statistical procedure. Using this methodology, several regions of GM volume reductions were detected in our HR sample compared to HC.

The most prominent alterations were identified bilaterally in 3 clusters of GM volume reductions covering the medial and lateral prefrontal cortices, as well as the orbitofrontal areas. The GM volume decrements in the frontal areas ranged between -1.8 and -2.8% for the left and between -1.6 and -4.3% for the right hemisphere. Additionally, large portions of the ACC showed GM volume reductions, bilaterally. Further structural alterations were detected in the caudate nuclei, the precentral gyri and supplementary motor areas. Using cross-sectional VBM, Job et al. (2003) compared GMD at the whole-brain level in 146 genetically predisposed subjects with 36 HC subjects by use of SPM99 at uncorrected and small-volume corrected significance levels. The small-volume correction revealed significant GMD reductions in the ACC but not in prefrontal areas. Pantelis et al. (2003a) applied a permutational VBM analysis using cluster-level statistics in a cross-sectional design. Twenty-three HR subjects that subsequently developed psychosis (converters) were compared with 52 non-converters. In the converter group the authors found baseline GM volume reductions in the right

ventrolateral prefrontal cortex at the statistical level of $P < 0.05$. Additionally, GM volume reductions were seen bilaterally in the ACC and on the right hemisphere within the hippocampus, parahippocampus and surrounding cortex. Similarly, Borgwardt et al. (2007) compared 35 HR subjects with 22 HC by means of cluster-level statistics. They showed GM volume reductions in the posterior cingulate gyrus and precuneus. Additional reductions emerged in the left insula and STG, left parahippocampus/hippocampus and in the amygdala, bilaterally. Finally, no differences in prefrontal regions were detected. Prefrontal abnormalities have been suggested to be a core structural alteration in schizophrenia, already present in first-episode patients (Steen et al., 2006; Vita et al., 2006). Fifteen (37.5%) out of 40 HR subjects finally developed a psychotic disorder with a mean time to onset of 188 days. This transition rate is in keeping with data previously presented by Yung et al. (2004) who reported a transition rate of 34.6% in their sample of 104 ultra-high risk subjects during the first 12 months of follow-up. Thus, our HR sample may be comparable with the ultra-high risk population of Yung et al. (2004) regarding the prevalence of an ultimate transition to psychosis. In this context, the prefrontal structural abnormalities found in HR compared to HC may not only be interpreted as specific markers of an elevated susceptibility to basic symptoms, attenuated psychotic symptoms or brief limited intermittent psychotic symptoms but also as markers of the prodromal phase of psychosis.

The prevalence of first-degree relatives with psychiatric diseases was not significantly different between the subjects with and without subsequent disease manifestation. Furthermore, no significant differences were observed between the converters and non-converters with respect to pre- and perinatal complications. Genetic loading and obstetric complications in the converter group were higher, although not significantly. This may be due to the small sample sizes of the each subgroup. Both aspects seem to be key variables in developing psychosis and, in fact a positive family history of psychosis has been the key intake criterion of genetically defined HR samples (Johnstone et al., 2000).

Furthermore, we detected significant correlations between GM volume and the PANSS positive and negative scores localized within the prefrontal brain areas of our HR subjects. Positive symptoms were inversely correlated with GM volume in a cluster covering the DMPFC, bilaterally as well as the left ACC. Spatially extended alterations were found to be inversely correlated with the severity of the PANSS negative scores covering the medial prefrontal regions, bilaterally, as well as the left DLPFC and VLPFC.

In contrast to our findings, Spencer et al. observed positive correlations between the severity of positive symptoms (hallucinations and delusions) and GMD within the left STG of genetically predisposed HR subjects (Spencer et al., 2007). In their study, the severity of anxiety was positively correlated with GMD in the right dorsomedial thalamic nucleus and inversely correlated with GMD in the left parahippocampus and hippocampus. Our results may not be directly comparable to their findings as our HR sample was recruited by following a “close-in” strategy (Yung et al., 2004) in contrast to their HR population defined by an enhanced risk of psychosis due to intellectual disability. Moreover, Spencer et al. used the Clinical Interview Schedule (Krawiecka et al., 1977), which in contrast to the PANSS may measure different aspects of prodromal symptomatology. Nevertheless, our correlational VBM results may emphasize an important role of the prefrontal cortex in the emergence of prodromal symptoms. Furthermore, our findings of a linear relationship between lateral prefrontal brain alterations and negative symptoms are in keeping with our recent VBM study showing prominent prefrontal alterations in schizophrenic patients with predominant negative symptoms (Koutsouleris et al., 2008) and the VBM findings of Sigmundsson et al. (2001). Finally, our data may support to further investigate the pathophysiology of emerging negative symptoms in the prodromal phase of psychosis (Lencz et al., 2004).

In our HR sample, further GM volume reductions were detected in the temporal, parietal and frontal portions of the left perisylvian structures as well as in the left insular cortex. Using a cluster-size threshold of $P < 0.05$ (5.2 cm^3), FWE-corrected, we did not find an involvement of the medial temporal structures. Our perisylvian results are in line with the findings from our own recent study of 175 schizophrenic patients compared to 177 HC (Koutsouleris et al., 2008) and a recent meta-analysis (Honea et al., 2005) summarizing 15 VBM studies with a total of 390 first-episode and chronic schizophrenic patients. Furthermore, our data is consistent with the results of Pantelis et al. (2003a) who reported structural alterations of the right STG and the inferior frontal gyrus in HR subjects versus HC. Borgwardt et al. (2007) showed focal GM volume reductions in their entire HR sample within the left insula and bilaterally in the STG compared to HC. In his converter sample again the ACC, the right STG and insula were affected.

Our negative findings regarding the medial temporal lobe structures are in contrast with Pantelis et al. (2003a) who detected GM volume reductions in the right hippocampal and parahippocampal region of HR subjects. Also Job et al. (2003) showed similar alterations in the left parahippocampal regions. In keeping with this data,

Borgwardt et al. (2007) detected GM volume reductions in the left medial temporal structures, including the hippocampus, parahippocampus and amygdala in HR subjects compared to HC. However, in a recent publication Velakoulis et al. (2006) reported non-reduced hippocampus and amygdala volumes in a large sample of 135 HR subjects compared to 87 HC using region-of-interest measurements. Moreover, Phillips et al. reported a non-reduction of hippocampus volume in HR subjects who subsequently transitioned to psychosis compared to those HR subjects without disease manifestation and respective to HC (Phillips et al., 2002). Alterations of the medial temporal regions in schizophrenia are one of the most prominent reductions revealed by structural imaging research so far. Wright et al. (2000) reported structural reductions in the hippocampus/parahippocampus, with mean volume reductions of 5% to 8% in schizophrenic patients compared to controls. The heterogeneity of limbic findings in the current high-risk literature including our own negative results in the limbic brain regions may be interpreted (1) as a consequence of an increased *sample heterogeneity* in currently available HR populations which is due to the fact that some HR subjects develop psychosis whereas others do not, and/or (2) as the results of *dynamic neuroanatomical changes* during the high-risk state that do not only involve GM reductions but also transient GM increases in interconnected brain regions (see Phillips et al., 2002; Borgwardt et al., 2007; Spencer et al. 2007, for a discussion).

Finally, the present study employed the new unified segmentation algorithms of SPM5. To our knowledge, this is the first study applying this new VBM methodology to the investigation of morphometric abnormalities in HR populations. With the extensions provided by the VBM5 toolbox the new algorithms may improve normalization to standard space, which has frequently been criticized for yielding insufficient results in SPM99 and SPM2 (Davatzikos, 2004).

In summary, GM volume reductions were observed in our HR sample within the prefrontal and temporal brain regions. Our data suggest that the vulnerable high-risk state is associated with structural brain alterations, similar to the structural reductions seen in the first and recurrent episode state of schizophrenia. Prospective longitudinal follow-up research in our sample is required to evaluate the structural biomarkers that indicate a subsequent transition to psychosis.

Role of funding source

Funding was provided by the Ministry of Education and Science (BMBF) of the Federal Republic of Germany for the multi-center high-risk study conducted within the German Research Network for

Schizophrenia. The BMBF had no further role in study design; in the collection, analysis and interpretation of data; in the writing of the report; and in the decision to submit the paper for publication.

Contributors

Author Eva Meisenzahl designed the study, participated in the collection of clinical and MRI data, evaluated the results of statistical analysis and wrote the manuscript.

Author Nikolaos Koutsouleris participated in the collection of clinical and MRI data, performed the data processing and statistical analysis, participated in the evaluation and discussion of results and the writing of the manuscript.

Author Christian Gaser supervised data processing and statistical analysis.

Author Gisela Schmitt participated in the acquisition of data, the evaluation of results and the writing of the manuscript.

Author Ronald Bottlender was responsible for the recruitment of HR subjects and the acquisition of clinical data, and participated in the evaluation of results and the writing of the manuscript.

Author Petra Decker participated in the recruitment of HR subjects and the acquisition of clinical data.

Author Bernhard Burgermeister supervised data analysis and participated in writing the manuscript.

Author Christine Born participated in MRI data acquisition.

Author Hans-Jürgen Möller supervised the evaluation and discussion of scientific results and the writing of the manuscript.

Conflict of interest

No conflict of interest exists for any of the authors.

Acknowledgements

We would like to thank the staff of our Early Intervention Program who were responsible for the recruitment and examination of high-risk individuals. Furthermore, we would like to thank all healthy volunteers who participated in our study for their valuable and indispensable contribution to our research field.

References

- Andreasen, N.C., 1999. A unitary model of schizophrenia: Bleuler's "fragmented phrene" as schizencephaly. *Arch. Gen. Psychiatry* 56, 781–787.
- Ashburner, J., Friston, K.J., 2000. Voxel-based morphometry—the methods. *Neuroimage* 11, 805–821.
- Ashburner, J., Friston, K.J., 2005. Unified segmentation. *Neuroimage* 26, 839–851.
- Bach Cuadra, M., Cammoun, L., Butz, T., Cuisenaire, O., Thiran, J.P., 2005. Comparison and validation of tissue modelization and statistical classification methods in T1-weighted MR brain images. *IEEE Trans. Med. Imag.* 24, 1548–1565.
- Benes, F.M., 1991. Evidence for neurodevelopment disturbances in anterior cingulate cortex of post-mortem schizophrenic brain. *Schizophr. Res.* 5, 187–188.
- Borgwardt, S.J., Riecher-Rössler, A., Dazzan, P., Chitnis, X., Aston, J., Drewe, M., Gschwandtner, U., Haller, S., Pflger, M., Rechsteiner, E., D'Souza, M., Stieglitz, R.-D., Rad, E.-W., McGuire, P.K., 2007. Regional gray matter volume abnormalities in the at risk mental state. *Biol. Psychiatry* 61, 1148–1156.

- Cao, J., Worsley, K.J., 2001. Application of random fields in human brain mapping. In: Moore, M. (Ed.), *Spatial Statistics: Methodological Aspects and Applications*. Springer Lecture Notes in Statistics, pp. 169–182.
- Davatzikos, C., 2004. Why voxel-based morphometric analysis should be used with great caution when characterizing group differences. *Neuroimage* 23, 17–20.
- Good, C.D., Johnsrude, I.S., Ashburner, J., Henson, R.N., Friston, K.J., Frackowiak, R.S., 2001. A voxel-based morphometric study of ageing in 465 normal adult human brains. *Neuroimage* 14, 21–36.
- Häfner, H., Maurer, K., Ruhrmann, S., Bechdolf, A., Klosterkötter, J., Wagner, M., Maier, W., Bottlender, R., Möller, H.-J., Gaebel, W., Wölwer, W., 2004. Early detection and secondary prevention of psychosis: facts and visions. *Eur. Arch. Psychiatry Clin. Neurosci.* 254, 117–128.
- Hayasaka, S., Phan, K.L., Liberzon, I., Worsley, K.J., Nichols, T.E., 2004. Nonstationary cluster-size inference with random field and permutation methods. *Neuroimage* 22, 676–687.
- Honea, R., Crow, T.J., Passingham, D., Mackay, C.E., 2005. Regional deficits in brain volume in schizophrenia: a meta-analysis of voxel-based morphometry studies. *Am. J. Psychiatry* 162, 2233–2245.
- Job, D.E., Whalley, H.C., McConnell, S., Glabus, M., Johnstone, E.C., Lawrie, S.M., 2003. Voxel-based morphometry of grey matter densities in subjects at high risk of schizophrenia. *Schizophr. Res.* 64, 1–13.
- Job, D.E., Whalley, H.C., Johnstone, E.C., Lawrie, S.M., 2005. Grey matter changes over time in high risk subjects developing schizophrenia. *Neuroimage* 25, 1023–1030.
- Johnstone, E., Abukmeil, S., Byrne, M., Clafferty, R., Grant, E., Hodges, A., Lawrie, S., Owens, D., 2000. Edinburgh high risk study — findings after four years: demographic, attainment and psychopathological issues. *Schizophr. Res.* 46, 1–15.
- Klosterkötter, J., Hellmich, M., Steinmeyer, E.M., Schultze-Lutter, F., 2001. Diagnosing schizophrenia in the initial prodromal phase. *Arch. Gen. Psychiatry* 58, 158–164.
- Kojoh, K., Hirasawa, S., 1990. The Bonn Scale for the Assessment of Basic Symptoms (BSABS). *Arch. Psychiatr. Diagn. Clin. Eval.* 4, 587–597.
- Koutsouleris, N., Gaser, C., Jäger, M., Bottlender, R., Frodl, T., Holzinger, S., Schmitt, G.J.E., Zetsche, T., Burgermeister, B., Scheuerecker, J., Born, C., Reiser, M., Möller, H.-J., Meisenzahl, E.M., 2008. Structural correlates of psychopathological symptom dimensions in schizophrenia: a voxel-based morphometric study. *Neuroimage* 39, 1600–1612.
- Krawiecka, M., Goldberg, D., Vaughan, M., 1977. A standardized psychiatric assessment scale for rating chronic psychotic patients. *Acta Psychiatr. Scand.* 55, 299–308.
- Lawrie, S.M., Whalley, H., Kestelman, J.N., Abukmeil, S.S., Byrne, M., Hodges, A., Rimmington, J.E., Best, J.J., Owens, D.G., Johnstone, E.C., 1999. Magnetic resonance imaging of brain in people at high risk of developing schizophrenia. *Lancet* 353, 30–33.
- Lehrl, S., 2005. *Mehrfachwahl-Wortschatz-Intelligenztest MWT-B*. Balingen, Spitta Verlag.
- Lenz, T., Smith, C.W., Auther, A., Correll, C.U., Comblatt, B., 2004. Nonspecific and attenuated negative symptoms in patients at clinical high-risk for schizophrenia. *Schizophr. Res.* 68, 37–48.
- McGlashan, T.H., Hoffman, R.E., 2000. Schizophrenia as a disorder of developmentally reduced synaptic connectivity. *Arch. Gen. Psychiatry* 57, 637–648.
- McIntosh, A.M., Baig, B.J., Hall, J., Job, D., Whalley, H.C., Lymer, G.K.S., Moorhead, T.W.J., Owens, D.G.C., Miller, P., Porteous, D., Lawrie, S.M., Johnstone, E.C., 2007. Relationship of catechol-*O*-methyltransferase variants to brain structure and function in a population at high risk of psychosis. *Biol. Psychiatry* 61, 1127–1134.
- Nichols, T.E., Holmes, A.P., 2002. Nonparametric permutation tests for functional neuroimaging: a primer with examples. *Hum. Brain Mapp* 15, 1–25.
- Pantelis, C., Velakoulis, D., McGorry, P.D., Wood, S.J., Suckling, J., Phillips, L.J., Yung, A.R., Bullmore, E.T., Brewer, W., Soulsby, B., Desmond, P., McGuire, P.K., 2003a. Neuroanatomical abnormalities before and after onset of psychosis: a cross-sectional and longitudinal MRI comparison. *Lancet* 361, 281–288.
- Pantelis, C., Yücel, M., Wood, S.J., McGorry, P.D., Velakoulis, D., 2003b. Early and late neurodevelopmental disturbances in schizophrenia and their functional consequences. *Aust. N. Z. J. Psychiatry* 37, 399–406.
- Pantelis, C., Yücel, M., Wood, S.J., Velakoulis, D., Sun, D., Berger, G., Stuart, G.W., Yung, A., Phillips, L., McGorry, P.D., 2005. Structural brain imaging evidence for multiple pathological processes at different stages of brain development in schizophrenia. *Schizophr. Bull.* 31, 672–696.
- Phillips, L.J., Yung, A.R., Yuen, H.P., Pantelis, C., McGorry, P.D., 2002. Prediction and prevention of transition to psychosis in young people at incipient risk for schizophrenia. *Am. J. Med. Genet.* 114, 929–937.
- Poline, J.B., Worsley, K.J., Evans, A.C., Friston, K.J., 1997. Combining spatial extent and peak intensity to test for activations in functional imaging. *Neuroimage* 5, 83–96.
- Sigmundsson, T., Suckling, J., Maier, M., Williams, S., Bullmore, E., Greenwood, K., Fukuda, R., Ron, M., Toone, B., 2001. Structural abnormalities in frontal, temporal, and limbic regions and interconnecting white matter tracts in schizophrenic patients with prominent negative symptoms. *Am. J. Psychiatry* 158, 234–243.
- Spencer, M.D., Moorhead, T.W.J., McIntosh, A.M., Stanfield, A.C., Muir, W.J., Hoare, P., Owens, D.G.C., Lawrie, S.M., Johnstone, E.C., 2007. Grey matter correlates of early psychotic symptoms in adolescents at enhanced risk of psychosis: a voxel-based study. *Neuroimage* 35, 1181–1191.
- Steen, R.G., Mull, C., McClure, R., Hamer, R.M., Lieberman, J.A., 2006. Brain volume in first-episode schizophrenia: systematic review and meta-analysis of magnetic resonance imaging studies. *Br. J. Psychiatry* 188, 510–518.
- Tzourio-Mazoyer, N., Landeau, B., Papathanassiou, D., Crivello, F., Etard, O., Delcroix, N., Mazoyer, B., Joliot, M., 2002. Automated anatomical labeling of activations in SPM using a macroscopic anatomical parcellation of the MNI MRI single-subject brain. *Neuroimage* 15, 273–289.
- Velakoulis, D., Wood, S.J., Wong, M.T., McGorry, P.D., Yung, A., Phillips, L., Smith, D., Brewer, W., Proffitt, T., Desmond, P., Pantelis, C., 2006. Hippocampal and amygdala volumes according to psychosis stage and diagnosis: a magnetic resonance imaging study of chronic schizophrenia, first-episode psychosis, and ultra-high-risk individuals. *Arch. Gen. Psychiatry* 63 (2), 139–149.
- Vita, A., Peri, L.D., Silenzi, C., Dieci, M., 2006. Brain morphology in first-episode schizophrenia: a meta-analysis of quantitative magnetic resonance imaging studies. *Schizophr. Res.* 82, 75–88.
- Weinberger, D.R., 1987. Implications of normal brain development for the pathogenesis of schizophrenia. *Arch. Gen. Psychiatry* 44, 660–669.
- Worsley, K.J., Andermann, M., Koulis, T., MacDonald, D., Evans, A.C., 1999. Detecting changes in nonisotropic images. *Hum. Brain Mapp* 8, 98–101.
- Wright, I.C., Rabe-Hesketh, S., Woodruff, P.W., David, A.S., Murray, R.M., Bullmore, E.T., 2000. Meta-analysis of regional brain volumes in schizophrenia. *Am. J. Psychiatry* 157, 16–25.

- Yücel, M., Wood, S.J., Fornito, A., Riffkin, J., Velakoulis, D., Pantelis, C., 2003. Anterior cingulate dysfunction: implication for psychiatric disorders? *Rev. Psychiatr. Neurosci.* 28, 350–354.
- Yung, A.R., Phillips, L.J., McGorry, P.D., McFarlane, C.A., Francey, S., Harrigan, S., Patton, G.C., Jackson, H.J., 1998. Prediction of psychosis. A step towards indicated prevention of schizophrenia. *Br. J. Psychiatr., Suppl.* 172, 14–20.
- Yung, A.R., Phillips, L.J., Yuen, H.P., Francey, S.M., McFarlane, C.A., Hallgren, M., McGorry, P.D., 2003. Psychosis prediction: 12-month follow up of a high-risk (“prodromal”) group. *Schizophr. Res.* 60, 21–32.
- Yung, A.R., Phillips, L.J., Yuen, H.P., McGorry, P.D., 2004. Risk factors for psychosis in an ultra high-risk group: psychopathology and clinical features. *Schizophr. Res.* 67, 131–142.